



TEKSTİL VE MÜHENDİS
(Journal of Textiles and Engineer)



<http://www.tekstilvemuhendis.org.tr>

PRODUCTION AND CHARACTERIZATION OF PHB, PHBV ELECTROSPUN FIBERS AND THEIR BLENDS

PHB, PHBV VE KARIŞIMI ELEKTRO ÇEKİM LİFLERİN ÜRETİMİ VE KARAKTERİZASYONU

Hatice Aybige AKDAĞ ÖZKAN^{1,2*}
Şebnem DÜZYER GEBİZLİ^{1,3}
Aslı HOCKENBERGER^{1,3}

¹Bursa Uludag University Graduate School of Natural and Applied Sciences, Bursa, Turkey

²KORTEKS Mensucat Sanayi ve Ticaret A.Ş., Polymeric Materials Department Bursa, Turkey

³Bursa Uludag University, Textile Engineering Department Bursa, Turkey




Online Erişime Açıldığı Tarih (Available online):30 Eylül 2023 (30 September 2023)

Bu makaleye atıf yapmak için (To cite this article):

Hatice Aybige AKDAĞ ÖZKAN, Şebnem DÜZYER GEBİZLİ, Aslı HOCKENBERGER (2023):
Production And Characterization Of Phb, Phbv Electrospun Fibers And Their Blends, Tekstil ve
Mühendis, 30: 131, 171- 179.

For online version of the article: <https://doi.org/10.7216/teksmuh.1268253>

PRODUCTION AND CHARACTERIZATION OF PHB, PHBV ELECTROSPUN FIBERS AND THEIR BLENDS

Hatice Aybige AKDAĞ ÖZKAN^{1,2*} 
Şebnem DÜZYER GEBİZLİ^{1,3} 
Aslı HOCKENBERGER^{1,3} 

¹Bursa Uludag University Graduate School of Natural and Applied Sciences, Bursa, Turkey
²KORTEKS Mensucat Sanayi ve Ticaret A.Ş., Polymeric Materials Department Bursa, Turkey
³Bursa Uludag University, Textile Engineering Department Bursa, Turkey

Gönderilme Tarihi / Received: 06.04.2023
Kabul Tarihi / Accepted: 15.09.2023

ABSTRACT: Polhydroxybutyrates (PHBs) are well-known bio-based and biodegradable bacterial polyesters. In this study, the effects of polymer type, solution concentration and feeding rate on the electrospinnability of Poly(3-hydroxybutyrate) (PHB) and Poly(3-hydroxybutyrate-co-3-hydroxyvalerate) PHBV nanofibers were investigated. First, PHB, PHBV and PHB/PHBV solutions with different polymer concentrations ranging between 5-11% wt. were prepared and characterized in terms of viscosity. Afterwards, electrospinning was performed and ultrafine fibers were produced. The surface morphology and the fiber diameters of the samples were investigated by scanning electron microscopy (SEM) analyses. Pore sizes of the samples were also calculated. In order to understand the wettability of the samples, contact angle measurements were conducted. The thermal properties and the crystallinity of the samples were investigated differential scanning calorimetry (DSC) analyses. The solution viscosities increased dramatically above %9 wt. of polymer concentration. SEM images revealed that decreasing feeding rate and increasing solution concentration resulted in fewer bead formation. On the other hand, fibers with diameters from 1.2 to 5.4 μm were produced with the increasing solution concentration and increasing voltage. All samples showed contact angle values above 90° indicating that they are hydrophobic. The PHB/PHBV blend surface showed the highest contact angle. DSC analyses showed that PHBV surface had significantly lower crystallization degree than PHB surface produced at the same concentration. It can be concluded that PHB fibers can be successfully produced by electrospinning.

Key words: Biopolymer, polyhydroxybutyrate, bacterial polyester, electrospinning

PHB, PHBV VE KARIŞIMI ELEKTRO ÇEKİM LİFLERİN ÜRETİMİ VE KARAKTERİZASYONU

ÖZ: Polihidroksibütiratlar (PHB), biyobazlı ve biyolojik olarak parçalanabilen bakteriyel poliesterlerdir. Bu çalışmada, polimer tipi, çözelti konsantrasyonu, besleme oranı gibi proses parametrelerinin poli(3-hidroksibütirat) (PHB) ve Poli(3-hidroksibütirat-co-valerat) (PHBV) nanoliflerinin elektroçekimle üretilebilirliği üzerindeki etkileri incelenmiştir. İlk olarak, PHB, PHBV ve PHB/PHBV'den elektroçekim ile ağırlıkça %5-11 aralığında polimer içeren çözeltiler hazırlanmış ve viskoziteleri ölçülmüştür. Daha sonra elektro çekim prosesi ile ultra ince lifler üretilmiştir. Numunelerin yüzey morfolojileri, lif çapları ve gözenek boyutları taramalı elektron mikroskopu (SEM) ile incelenmiştir. Islanabilirliği anlamak için temas açısı ölçümleri yapılmıştır. Numunelerin termal özellikleri ve kristaliniteleri diferansiyel taramalı kalorimetri (DSC) analizleri ile incelenmiştir. Çözeltideki polimer konsantrasyonunun %9 üzerine çıkması çözelti konsantrasyonunu arttırmıştır. SEM görüntüleri, azalan besleme hızı ve artan çözelti konsantrasyonunun daha az boncuk oluşumuyla sonuçlandığını ortaya çıkarmıştır. Öte yandan, artan çözelti konsantrasyonu ve artan voltaj ile birlikte çapları 1,2-5,4 μm aralığında değişen lifler üretilmiştir. Tüm numuneler, 90°'nin üzerinde temas açısı değerleri göstererek hidrofobik karakter sergilemiştir. Bu numuneler arasında, PHB/PHBV karışımından elde edilen yüzey en yüksek temas açısını vermiştir. DSC analizleri, PHBV yüzeyinin aynı konsantrasyonda üretilen PHB yüzeyine göre önemli ölçüde daha düşük kristallenme derecesine sahip olduğunu göstermiştir. Bu sonuçlar doğrultusunda PHB liflerinin elektro çekim ile başarılı bir şekilde üretilebileceği sonucuna varılabilir.

Anahtar kelimeler: Biyopolimer, polihidroksibütirat, bakteriyel poliester, elektro çekim

*Sorumlu Yazarlar/Corresponding Author: aybigeakdag@uludag.edu.tr

DOI: <https://doi.org/10.7216/tekstilmuh.1268253>

www.tekstilmuhendis.org.tr

1. INTRODUCTION

Biodegradable polymers have gained attraction with the increasing demand for lowering the environmental damage and reducing conventional pollution. Among many biopolymers, Polyhydroxyalkonate (PHA) have potential in a wide range of applications with their bio-based, biodegradable and fast composting properties [1]. PHAs are synthesized by microorganisms as a feed stock that polyester core inclusions which are surrounded by phospholipids [2]. During the industrial production of PHA, process is started with fermentation and then, the polymer is extracted from cell debris, purified, and pellets are processed [3]. Polyhydroxybutyrate P(3HB) is a highly crystalline thermoplastic polymer which is the most common form of PHAs [1,3]. The type of PHA varies depending on the amount and type of carbon source in the environment. For instance, the addition of propionic acid or valeric acid to the glucose-containing growth medium leads to the production of a copolymer of 3-hydroxybutyrate (3HB) and 3-hydroxyvalerate (3HV) [3]. As a result of their large spherulites with low density and high crystallinity of PHAs, the weakest point is the low deformation at break, and brittleness [4]. The existence of 3HV in Polyhydroxybutyrate-co-valerate (PHBV) copolymer results in more flexible polymer with lower crystallinity [5]. Related to this assumption, PHB blends with PHBV to achieve better processability, degradation rate and mechanical properties [6,7].

Electrospinning is a versatile method for obtaining ultrafine [8] fibers in the micro and nano-range [9,10]. These method presents surfaces with high specific surface area, small pore and high porosity. The pores are fully interconnected to form a three-dimensional network and it is one of the most important parameters in determining the membrane's performance [9,10]. For instance, in filtration, the selectivity and separation efficiency of the membrane as well as the pressure drop across the filter are determined by the pore size distribution [11]. Electrospun surfaces make ground in many technical applications from medical products such as tissue scaffolds, drug delivery, to industrial products such as filtration and nano-electronics [7-14]. The electrospinning of ultrafine fibers depends on multiple parameter process, which is determined by structure of every single fiber, porosity, thickness, orientation etc. Electrospinning process parameters are mostly defined as three groups: solution parameters (viscosity, polymer type and concentration, solvent type, surface tension, etc.), process parameters (voltage, feeding rate, nozzle diameter, distance between the nozzle and the collector, collector type and speed, etc.) and environmental conditions (temperature, humidity, atmosphere type, etc.) [8]. In the literature there are studies about solvents used in binary solvent system to enhance morphology of electro spun mats [15,16]. If the feed rate is increased, there is an increase in fiber diameter or bead size, as more solution is drawn from the nozzle tip [14]. Effect of increasing feeding rate on fiber formation was showed at the paper which studied morphology of ultrafine

polysulfone fibers. Uniform fibers formed when the flow rate reduced from 0,66 to 0,44 mL/h [17]. Feeding rate is considered as one of the significant parameters to initiate the droplet shape, prolongation of Taylor cone, the track of the jet, and formation of bead free fiber [18].

Several studies were carried out on electrospinning process parameters of PHB, PHBV and their blends for various applications and effect of applied voltage and concentration of solution on surfaces were indicated [18-21]. However, studies about the effect of process parameters on fiber formation are restricted especially in feeding rate. In this study, we prepared solutions of industrial scale pellet form PHB, PHBV and their blends and investigated effects of polymer concentration, feeding rate, and applied voltage on the fiber formation and fiber properties to provide deeper insight for following studies.

2. MATERIALS AND METHODS

2.1. Materials

PHB pellets P309E (~600 kDa) and PHBV Enmat Y1000 (~400 kDa) (Hydroxyvalerate (HV) content was indicated to be around 3 % according to the data sheet) were supplied by Biomer (Germany) and Tianan Biologic (China), respectively. The pellets were dried at 60°C during an hour before using. Chloroform (Merck, TB: 61°C Solubility: 8 g/L (20°C)) and dichloromethane (DCM) (Sigma-Aldrich, TB: 39.8–40°C, Solubility: 13.2 g/L) were used as the solvent to dissolve the polymers.

2.2. Methods

In this study, PHB, PHBV and their blend solutions were prepared by dissolving the polymers in chloroform or chloroform/DCM solvent systems and stirred for 3h at 60 °C to obtain complete dissolution. (Table 1). The viscosities of the solutions were measured by a Brookfield RV-DV II viscometer according to ISO 2555 standard with 100 rpm. Afterwards, electrospinning was performed on an Inovenso NE300 electrospinning device. A single aluminum nozzle with 0.8 mm inner diameter was used and the distance between nozzle and rotating collector was kept at 15 cm. The fibers were collected on a drum with a rotating speed of 300 rpm. The parameters used in the study is given in Table 1. Electrospinning was performed from all solutions except S16 because of its high viscosity resulting in the clogging of the nozzle. All experiments were conducted at (25±2°C)

The surface properties of the samples were analyzed by a Carl Zeiss AG-EVO 40 XVP scanning electron microscope (SEM) with 2500 and 500 magnifications. The samples were coated with gold/palladium prior to analyses. The average fiber diameters and the pore sizes were calculated on 500 magnification SEM images by using Image J software over 20 measurements. The SEM images were transferred into the ImageJ software and threshold tool was used to select the areas of pore size [22,23].

Table 1. The solution and electrospinning parameters followed in the study

Sample No	Polymer	Solvent	Concentration [%]	Feeding Rate [mL/h]	Voltage [kV]
S1	PHB	CF	11	1	20
S2	PHB	CF	7	1	20
S3	PHB	CF	9	1	20
S4	PHB	CF/DCM*	7	1	20
S5	PHB	CF/DCM*	7	0,7	17
S6	PHB	CF/DCM*	9	0,7	17
S7	PHB	CF/DCM*	11	0,7	17
S8	PHB	CF	9	0,7	15
S9	PHB	CF	11	0,7	15
S10	PHB	CF	11	0,7	20
S11	PHB	CF	5	0,7	17
S12	PHB	CF	7	0,7	17
S13	PHBV	CF	7	0,7	17
S14	PHBV	CF	9	0,7	17
S15	PHB/PHBV**	CF	7	0,7	17
S16	PHB	CF	13	-	-

*CF/DCM: 75:25

**PHB/PHBV: 90:10

The contact angles of the samples were measured using KSV-The Modular CAM 200 contact angle measurement system. A distilled water drop was dispersed on each sample using a micropipette; the image of each drop was captured by the camera connected with a computerbased image capture system. The images were captured as quickly as possible after water droplet was placed onto the sample surface, and photographed in less than 1 s. Three measurements were performed on each sample and the average values were recorded.

In order to determine the thermal properties of the samples differential scanning calorimetry (DSC) analyses were performed by a Mettler Toledo Stare System DSC 823E at Korteks A.Ş. The samples were ramped from room temperature to 200 °C with a scanning rate of 10 °C/min under nitrogen atmosphere (30 cm³/min).

3. RESULTS AND DISCUSSION

For an effective electrospinning process, to ensure the continuity of the elongated and stretched polymer jet with the effect of electrostatic forces, it is necessary to adjust the polymer viscosity, thus the polymer solution concentration, to provide the optimum polymer chain complexity. As it known that the polymer concentration, molecular mass, and viscosity of the polymer-solvent system are related with each other [24]. Table 2 shows the viscosities of the polymer solutions prepared with different polymer concentrations. It can be seen that, viscosity of the polymer solutions increased dramatically above the %9 concentration. The influence of viscosity on electrospun fibers surface morphology and fiber formation was reported by previous studies [25-28]. These studies showed the fewer bead formation with the increasing viscosity. It was reported that surface tension

could control surface properties with decreased polymer concentration/solution viscosity and as a result, beaded fibers were produced [28].

PHB surfaces were produced with an 7%, 9% and 11% concentrations and 0.7 and 1 mL/h feed rates at applied voltage of 20kV. (S1, S2, S3) However, for 11% concentration, only 0.7 mL/h feed rate was used (S10) as a proper fiber could not be obtained with 1 mL/h feed rate due to high viscosity. Since 20kV voltage is high, it was decided to work at lower voltage values due to multijet formations. Furthermore, it was decided to continue the experiments with a feed rate of only 0.7 mL/h, since too beaded, high agglomeration formation and thick fibers are produced at 1 mL/h and above feeding rates.

The influence of the concentration (%5, %7, %9 and %13) was investigated keeping constant the value of the applied voltage at 17 kV. There were problems with surface formation at too high and low concentrations due to the low voltage. Multi-beaded surfaces were obtained at 5% concentration and stable jets were not formed at 13% concentration due to increased viscosity.

Only 9% and 11% concentration values could be produced at 15 kV applied voltage. (S8, S9) On the surfaces produced with PHB polymer and CF solvent (S1, S2, S3, S8, S9, S10, S11, S12), beadless, non-agglomerated surfaces were produced except for S1, S2, S3 and S11. It is considered that the too low concentration for S11 caused a high bead formation.

The SEM images of the electrospun fibers can be seen at Fig. 1. Effect of feeding rate and solution viscosity on regular fiber formation was observed considerably at Fig.1. S1, S2, S3, S8 and S12. Fibers with diameters ranging between 1,2 and 5.5 µm were produced. Although all the PHB solutions were able to form fibers at the selected electrospinning conditions, intense beads and spindle-like defects were seen especially when the feeding rate is 1 mL/h and above. It's known that, as the feed rate is increased, the volume of solution from the nozzle increases and polymer jet deposits on the collector before solvent evaporates completely, therefore ends up with increases in beads. In addition to this, it was observed multi jetting caused an uncharacteristic decrease in the fiber diameters. It's known that multi jets are formed in high concentration and viscous solutions and very high electrical field applications [14].

In addition, the polymer jet accelerated under the influence of a high voltage and reached to the collector plate quickly [30,31,32]. The feeding rate of polymer solution increased, so average diameter of the fibers increased from 4.1 to 5.4 µm. However, effect of voltage on fiber diameter and morphology much debated. It was reported that the higher voltage induced not only larger diameter but also smaller diameter at previous studies and It was determined that polymer concentration was much more effective on fiber diameter and morphology [29]. It was observed that from S9 and S10, the diameter of the fibers was not significantly

changed with changing applied voltage. However, significant diameter change can be shown between S1-S2, S5-S7, and S2-S10 by comparison with S9-S10. Furthermore, it was observed that the voltage was less effective compared to solution concentration and feed rate in terms of fiber morphology. It was reported that, to produce electrospun fibers, one of the most influential variables was polymer solution concentration [29]. In order to investigate the effect of the solvents on morphology of electrospun fibers, the polymer was dissolved in a single solvent (CF), and a mixed solvent (CF/DCM). Although the mixed solvent had high polymer concentration, it allowed a decent electrospinning. Furthermore, finer fibers were compared to the given concentration. This result can be associated by the previous studies to the increase in viscosity and faster evaporation rate of the mixed solvent [33,34,35]. In addition, regular bead-free electrospun fibers with diameters between 1.7 μm and 3.3 μm were obtained from PHBV. The PHBV fiber mats had average pore size of 19 μm^2 . Although PHBV fibers did not show any beads, PHB/PHBV fibers showed small agglomerations and beads. As it is stated in the literature, increased electrical conductivity causes more significant stretching of the jet [36]. As mentioned by previous research, blending solutions of the PHB and PHBV increased the electrical conductivity [37]. Therefore, the greater electrical conductivity of the blend solution can result in this situation.

It can be also seen that the pore sizes were not affected significantly by the voltage. However, the pore sizes were increased with the increasing polymer concentration due to the increasing fiber diameter. The fiber diameter and pore size are considerable geometrical properties of electrospun surfaces that significantly affect product utilization [38].

The results of the contact angle measurements are shown in Fig. 2. S6, S8, S11, S12, S14, and S15, were preferred to analyze the wetting behavior of surfaces due to their smaller fiber diameter and bead-free or less beaded surface. It can be seen that the contact angles of the fiber mats are all over 90° indicating the hydrophobic structure. The fibrous form of electrospun materials presents hydrophobic characteristics due to its micro and nano-size surface roughness [9]. Bead-rich topography increases the discontinuities, therefore, beaded electrospun structures are considerably rougher than completely fibrous structures. For this reason, S11 and S15 could show higher contact angle. On the other hand, decreasing fiber diameter can increase hydrophobic behavior due to the rougher surface because of the smaller pore size [30]. Mixed solvent solution was not showed comparable wetting properties.

Table 2. Fiber diameters and pore sizes of electrospun mats

Sample No	Viscosity [cP]	Avg. Diameter [μm]	CV [%]	Avg. Pore Size [μm^2]	CV [%]
S1	121	4.32	12	72	67
S2	121	1.23	15	2.19	59
S3	193	2.39	25	9.19	83
S4	136	1.27	14	2.31	59
S5	135	1,32	31	2.25	45
S6	200	2,25	30	8.95	70
S7	1310	3,52	15	25	55
S8	210	3.37	26	74	61
S9	1200	4.16	19	84	56
S10	1200	5.44	27	131	85
S11	73	1.41	15	3.63	77
S12	112	2.59	19	30	62
S13	121	1.77	20	19	27
S14	219	3.31	19	106	59
S15	115	1.66	28	4.55	59
S16	1475	-	-	-	-

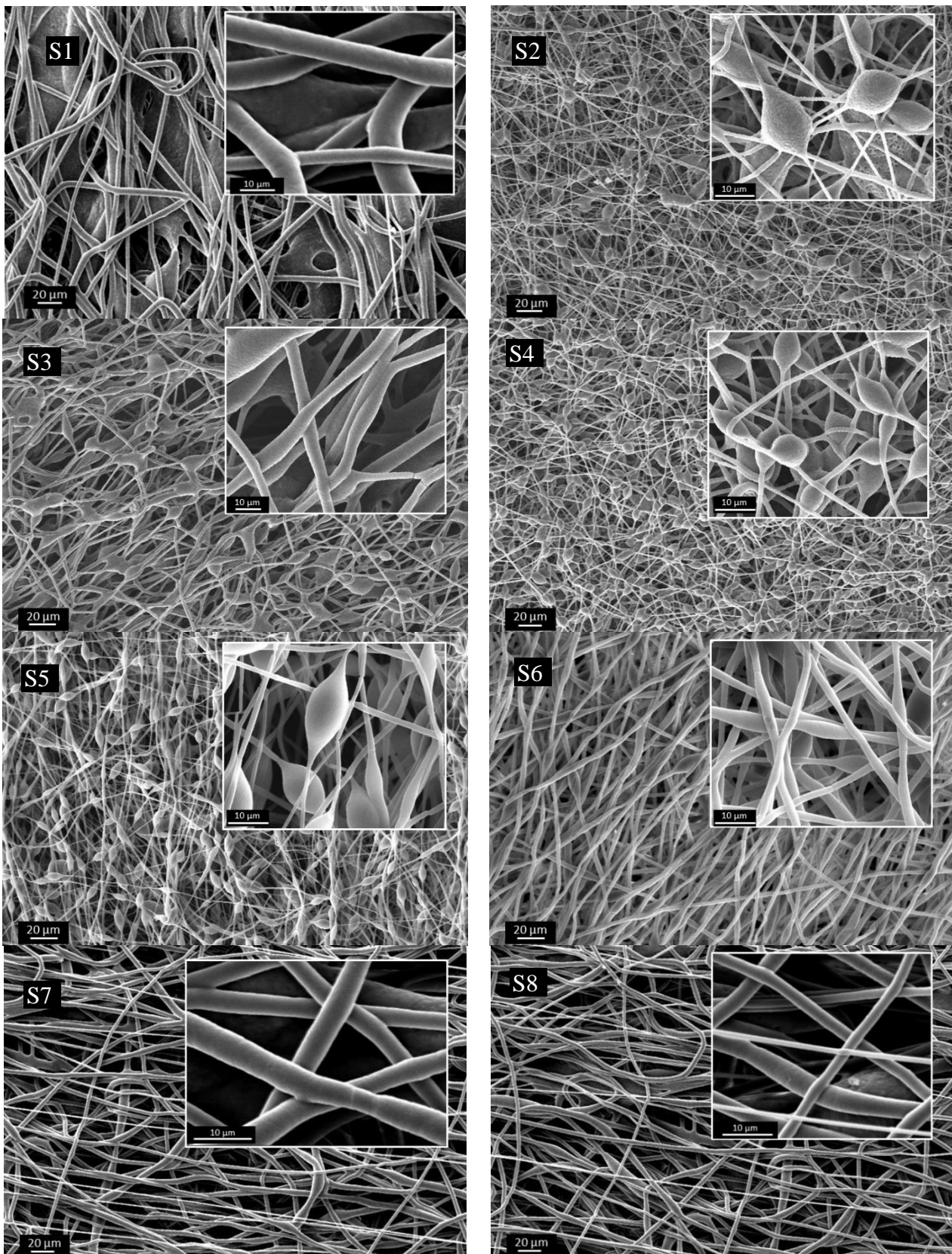


Figure 1. SEM images of electrospun mats at 500x (the inset images correspond to 2500x magnification)

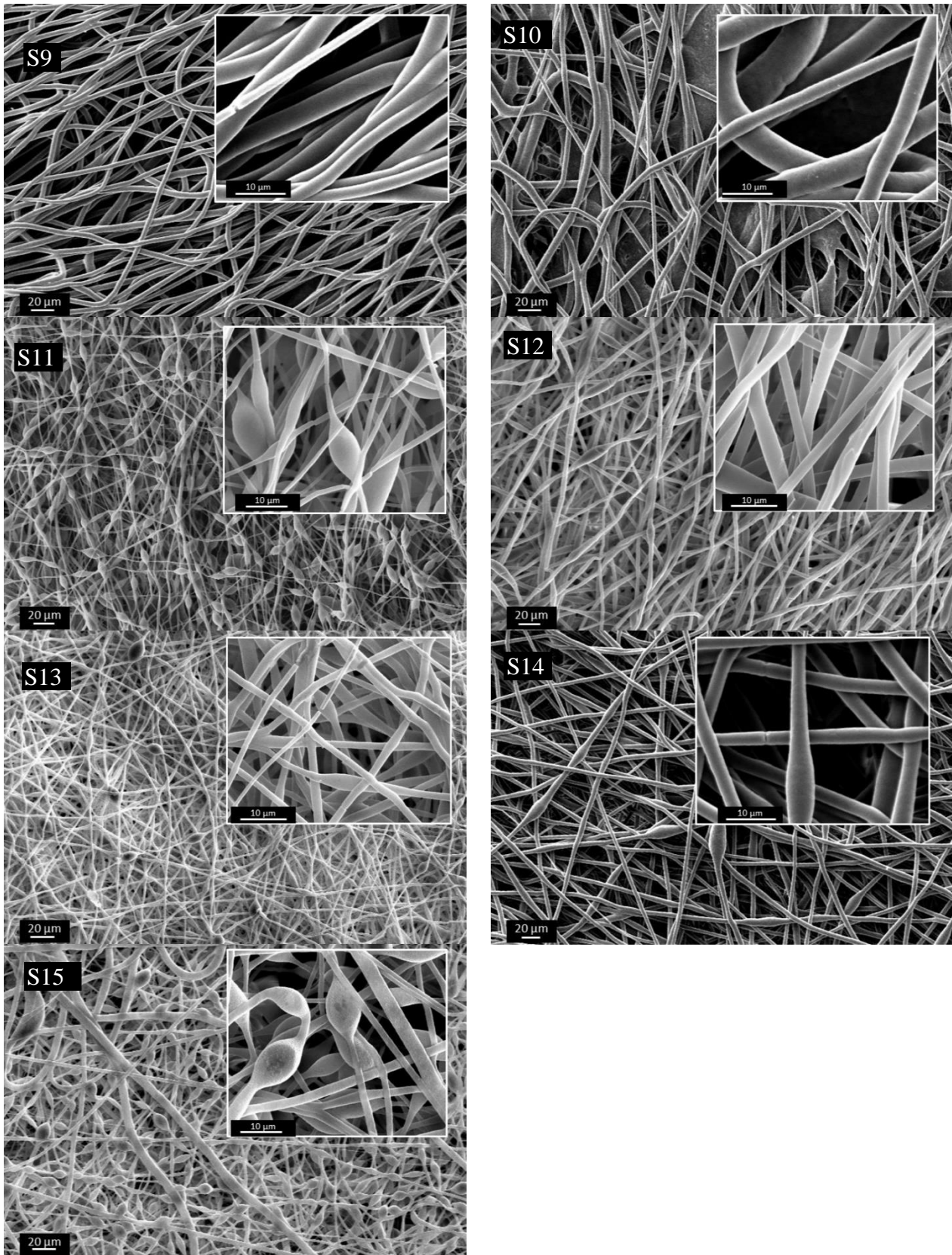


Figure 1. SEM images of electrospun mats at 500x (the inset images correspond to 2500x magnification)

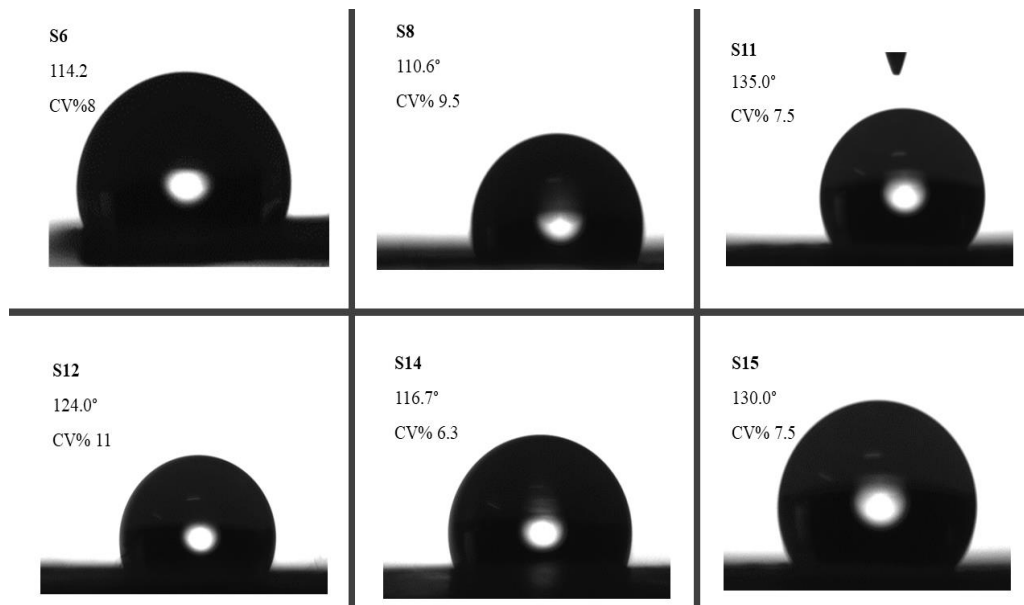


Figure 2. Contact angle values of the samples

The thermal properties of the samples were investigated by DSC analyses. For the analyses, four samples (S8-12-14 and 15) were selected to see the effect of polymer concentration and polymer type. In addition, the crystallinity of these samples was derived from the DSC thermograms. $T_{m, onset}$ is starting of the melting process and X_c is to observe the ability of the sample to crystallize when it was subjected to a constant cooling scan. The crystallinity of the surfaces was calculated on the basis of the heat of fusion for PHB. As it can be seen at Fig. 3 blends of P(3HB) with PHBV containing less than 10 mol% of 3HV are miscible according to previous study [38], so their thermograms didn't have two melting peaks. PHB, PHBV and their blends presented similar peaks. With the increasing concentration, a sharper peak with high melting enthalpy was detected. The melting temperature is related with more stable crystals. According to the DSC results from Fig. 4, PHBV was less crystalline than PHB due to the presence of the smaller number of valerate comonomer groups. Moreover, blending PHB with PHBV caused melting temperature to decrease whereas the crystallinity degree increased. These discrepancies can be based on process fluctuation of samples.

Table 3. DSC results of electrospun PHB surface

Sample No	$T_{m, onset}$ [°C]	$T_{m, peak}$ [°C]	T_c [°C]	ΔH_m [J/g]	ΔH_c [J/g]	X_c^* [%]
S8	162	173	95	81	72	48
S12	160	173	79	79	81	44
S14	162	173	118	80	83	26
S15	155	170	109	72	69	52

* X_c : degree of crystallinity, calculated from $\Delta H_f / \Delta H^0_f$ (ΔH^0_f : 146.6 J/g).

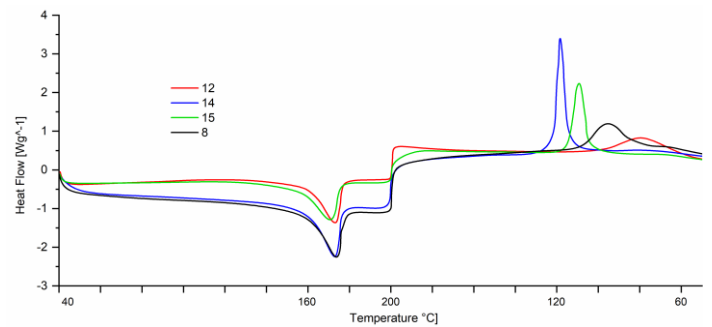


Figure 3. DSC thermograms of the electrospun surfaces

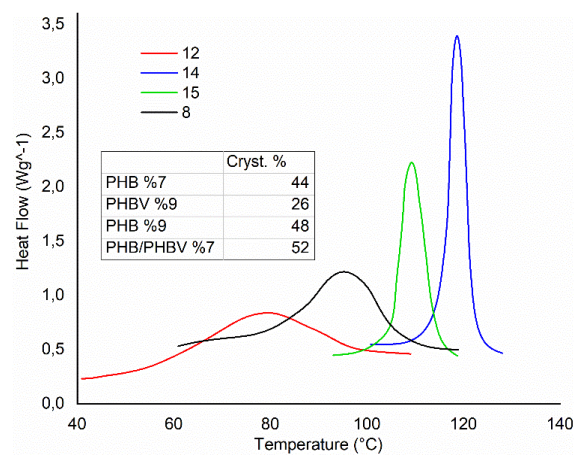


Figure 4. DSC thermograms and crystallization degrees of the electrospun surfaces.

4. CONCLUSION

In this study, electrospun biodegradable ultrafine fibers were produced from PHB, PHBV and their blend solutions with different polymer concentrations. The effect of solution properties and process parameters on the fiber formation were investigated.

The viscosity measurements showed that the viscosity increases dramatically above 9 wt. of polymer concentration. It was also seen that the polymer solution with 13% wt. of polymer concentration could not be electrospun as a result of its high viscosity which leads to clogging of the nozzle.

SEM images revealed that beaded-fibers with diameters between 1.5-3 μm were produced from the solutions with low viscosities. With the increasing viscosity, the number of beads were lowered, and more uniform fibers were obtained. Above 9% wt. of polymer concentration, the fiber diameters were increased to 4-5.5 μm due to the increase in the viscosity. Besides, at the 13% wt. of polymer concentration the viscosity reached to a level that deteriorated processability. Moreover, it was seen that process parameters such as feeding rate and voltage are also effective on the fiber morphology. With higher feeding rates, there was not enough time for the solvent to evaporate and some solvent remained in the fibers on the collecting surface resulting in the sticking of the fibers at contact points. On the other hand, higher amount of polymer was withdrawn with the higher voltage and resulted in higher diameters and pore sizes. The average diameter of the fibers produced from the solutions containing CF/DCM were between 1.27 and 3.5 μm . The average fiber diameters of S4, S5, S6, and S7 were decreased significantly compared to S8, S9, and S12. The best jet formation was observed from the solutions containing CF/DCM. Electrospun surfaces with smaller diameter exhibited higher contact angles of around 130°. DSC thermograms showed that crystallinity of samples was similar except PHBV. Melting temperature and enthalpy didn't show a distinct alternation between samples indicating that constitutive polymers were not degraded during process.

The overall results indicate that PHB, PHBV and their blend fibers can be successfully electrospun. Solution and process parameters have significant effect on the fiber morphology. It can be concluded that for an effective electrospinning process, it is necessary to adjust the solution viscosity, hence the polymer solution concentration as well as the process parameters such as feeding rate and voltage.

Acknowledgement

This research was performed under the Industrial PhD Fellowship Program of Scientific and Technological Research Council of Turkey (TUBITAK) [118C040] in collaboration with Bursa Uludag University and KORTEKS, and supported by the Uludag University Scientific Research Projects Center (KUAB(MH)2020/15).

REFERENCES

- Koller, M., Salerno, A., Brauneegg, G (2013). *Bio-based plastics*. John Wiley & Sons Ltd, Chichester, p.137-140.
- Poli, A., Di Donato, P., Abbamondi, G. R., Nicolaus, B. (2011). Synthesis, production, and biotechnological applications of exopolysaccharides and polyhydroxyalkanoates by archaea. *Archaea*,
- Pollet, E., & Avérous, L. (2011). (Ed. Plackett, D.) *Biopolymers: new materials for sustainable films and coatings*. John Wiley & Sons, United Kingdom
- Chen, G.G-Q., (2005). (Ed. Smith, R.). *Biodegradable polymers for industrial applications*. Woodhead Publishing, USA
- Kootstra, A. M. J., Elissen, H. J. H., Huurman, S. (2017). *PHA's (Polyhydroxyalkanoates): General information on structure and raw materials for their production*, A running document for "Kleinschalige Bioraffinage WP9: PHA", Task 5 (No. 727). Wageningen UR, PPO/Acrres.
- Chan, C. H., Kummerlöwe, C., Kammer, H. W. (2004). *Crystallization and melting behavior of poly (3-hydroxybutyrate)-based blends*. *Macromolecular Chemistry and Physics*, 205(5), 664-675.
- Ublekov, F., Budurova, D., Staneva, M., Natova, M., Penchev, H. (2018). *Self-supporting electrospun PHB and PHBV/organoclay nanocomposite fibrous scaffolds*. *Materials Letters*, 218, 353-356.
- Wang, X. X., Yu, G. F., Zhang, J., Yu, M., Ramakrishna, S., Long, Y. Z. (2021). *Conductive polymer ultrafine fibers via electrospinning: Preparation, physical properties and applications*. *Progress in Materials Science*, 115, 100704.
- Teo, W. E., Ramakrishna, S. (2006). *A review on electrospinning design and nanofibre assemblies*. *Nanotechnology*, 17(14), R89.
- Garg, K., Sell, S. A., Bowlin, G. L. (2009). (Ed. Eichhorn, S. J., Hearle, J.W.S., Jaffe, M., Kikutani, T.) *Electrospinning and its influence on the structure of polymeric nanofibers*. In *Handbook of Textile Fibre Structure* (p. 460-483). Woodhead Publishing, Cornwall, UK.
- Krifa, M., Yuan, W. (2016). *Morphology and pore size distribution of electrospun and centrifugal forcespun nylon 6 nanofiber membranes*. *Textile Research Journal*, 86(12), 1294-1306.
- Düzyer, Ş. (2017). *Fabrication of electrospun poly (ethylene terephthalate) scaffolds: characterization and their potential on cell proliferation in vitro*. *Textile and Apparel*, 27(4), 334-341.
- Duzyer, S., Hockenberger, A., Zussman, E. (2011). *Characterization of solvent - spun polyester nanofibers*. *Journal of Applied Polymer Science*, 120(2), 759-769.
- Nicosia, A., Gioparda, W., Foksovicz-Flaczyk, J., Walentowska, J., Wesolek, D., Vazquez, B., Belosi, F. (2015). *Air filtration and antimicrobial capabilities of electrospun PLA/PHB containing ionic liquid*. *Separation and Purification Technology*, 154, 154-160
- Md Khan T, Md Mamun, A.A., Mia R., Xu, A., Rashid, M.M. (2021): Effect of Different Solvent Systems on Fiber Morphology and Property of Electrospun PCL Nano Fibers, *Tekstil ve Mühendis*, 28: 122, 61-76.
- El-Hadi, A. M., Al-Jabri, F. Y. (2016). Influence of electrospinning parameters on fiber diameter and mechanical properties of poly (3-hydroxybutyrate)(PHB) and polyanilines (PANI) blends. *Polymers*, 8(3), 97.
- Ramakrishna, S. (2005). *An introduction to electrospinning and nanofibers*. World scientific.
- Acevedo, F., Villegas, P., Urtuvia, V., Hermosilla, J., Navia, R. Seeger, M. (2018). *Bacterial polyhydroxybutyrate for electrospun fiber production*. *International journal of biological macromolecules*, 106, 692-697.

19. Olk'khov, A. A., Staroverova, O., Iordanskii, A., Zaikov, G. (2014). *Morphology of electrospun nanofibres of polyhydroxybutyrate*. In AIP Conference Proceedings, 1599(1), 558-561. American Institute of Physics.
20. El-Hadi, A. M., Al-Jabri, F. Y. (2016). *Influence of electrospinning parameters on fiber diameter and mechanical properties of poly (3-hydroxybutyrate)(PHB) and polyanilines (PANI) blends*. Polymers, 8(3), 97.
21. Mottin, A. C., Ayres, E., Oréface, R. L., Câmara, J. J. D. (2016). *What changes in poly (3-hydroxybutyrate)(PHB) when processed as electrospun nanofibers or thermo-compression molded film?*. Materials Research, 19, 57-66.
22. Hojat, N., Gentile, P., Ferreira, A. M., Šiller, L. (2023). *Automatic pore size measurements from scanning electron microscopy images of porous scaffolds*. Journal of Porous Materials, 30(1), 93-101.
23. ImageJ User Guide, 30-Analyze, <https://imagej.nih.gov/ij/docs/guide/146-30.html>, Erişim Tarihi: 05.07.2023
24. Halabalová, V., Šimek, L., Dostál, J., Bohdanecký, M. (2004). *Note on the relation between the parameters of the Mark-Houwink-Kuhn-Sakurada equation*. International Journal of Polymer Analysis and Characterization, 9(1-3), 65-75.
25. Fong, H., Chun, I., Reneker, D. H. (1999). *Beaded nanofibers formed during electrospinning*. Polymer, 40(16), 4585-4592.
26. Zeng, J., Haoqing, H., Schaper, A., Wendorff, J., Greiner, A. (2003). *Poly-L-lactide nanofibers by electrospinning – Influence of solution viscosity and electrical conductivity on fiber diameter and fiber morphology*. e-Polymers, 3(1), 009.
27. Ol'khov, A. A., Staroverova, O. V., Gol'dshtrakh, M. A., Khvatov, A. V., Gumargalieva, K. Z., Iordanskii, A. L. (2016). *Electrospinning of biodegradable poly-3-hydroxybutyrate. Effect of the characteristics of the polymer solution*. Russian Journal of Physical Chemistry B, 10, 830-838.
28. Sombatmankhong, K., Suwantong, O., Waleetorncheepsawat, S., Supaphol, P. (2006). *Electrospun fiber mats of poly (3 - hydroxybutyrate), poly (3 - hydroxybutyrate - co - 3 - hydroxyvalerate), and their blends*. Journal of Polymer Science Part B: Polymer Physics, 44(19), 2923-2933.
29. Thompson, C. J., Chase, G. G., Yarin, A. L., & Reneker, D. H. (2007). *Effects of parameters on nanofiber diameter determined from electrospinning model*. Polymer, 48(23), 6913-6922.
30. Garg, K., Bowlin, G. L. (2011). *Electrospinning jets and nanofibrous structures*. Biomicrofluidics, 5(1).
31. Reneker, D. H., Kataphinan, W., Theron, A., Zussman, E., Yarin, A. L. (2002). *Nanofiber garlands of polycaprolactone by electrospinning*. Polymer, 43(25), 6785-6794.
32. Tan, S. H., Inai, R., Kotaki, M., & Ramakrishna, S. (2005). *Systematic parameter study for ultrafine fiber fabrication via electrospinning process*. Polymer, 46(16), 6128-6134.
33. Qin, X., & Wu, D. (2012). *Effect of different solvents on poly (caprolactone)(PCL) electrospun nonwoven membranes*. Journal of thermal analysis and calorimetry, 107(3), 1007-1013.
34. Theron, S. A., Zussman, E., & Yarin, A. L. (2004). *Experimental investigation of the governing parameters in the electrospinning of polymer solutions*. Polymer, 45(6), 2017-2030.
35. El-Hadi, A. M., & Al-Jabri, F. Y. (2016). *Influence of electrospinning parameters on fiber diameter and mechanical properties of poly (3-hydroxybutyrate)(PHB) and polyanilines (PANI) blends*. Polymers, 8(3), 97.
36. Xue, J., Wu, T., Dai, Y., & Xia, Y. (2019). *Electrospinning and electrospun nanofibers: Methods, materials, and applications*. Chemical reviews, 119(8), 5298-5415.
37. Sombatmankhong, K., Sanchavanakit, N., Pavasant, P., Supaphol, P. (2007). *Bone scaffolds from electrospun fiber mats of poly (3-hydroxybutyrate), poly (3-hydroxybutyrate-co-3-hydroxyvalerate) and their blend*. Polymer, 48(5), 1419-1427.
38. Kadam, V. V., Wang, L., Padhye, R. (2018). *Electrospun nanofibre materials to filter air pollutants—A review*. Journal of Industrial Textiles, 47(8), 2266-2267.
39. Conti, D. S., Yoshida, M. I., Pezzin, S. H., Coelho, L. A. F. (2007). *Phase behavior of poly (3-hydroxybutyrate)/poly (3-hydroxybutyrate-co-3-hydroxyvalerate) blends*. Fluid Phase Equilibria, 261(1-2), 79-84.